

CHAPTER IV

RESULTS AND DISCUSSION

In this study, two main parts of the experiments were systematically carried out including batch synthesis and dissolution experiments of the resulting precipitates. Batch synthesis experiments were conducted in order to understand the most important effects of precipitating conditions on the precipitate properties. There were three systems involved in batch synthesis experiments, Ca-ATMP precipitation synthesis, Mg-ATMP precipitation synthesis and Ca-ATMP precipitation synthesis with the presence of magnesium ion. After batch synthesis part was completed, the dissolution rates of the resulting precipitates were investigated by using a rotating disk reactor to evaluate the dissolution performance of each precipitates. The experimental data were shown in Appendix.

4.1 Characteristic of Synthesized Precipitates

4.1.1 Ca-ATMP Precipitates

This part was conducted to reproduce Ca-ATMP precipitates described in the previous work (Rerkpattanapipat, 1996). The previous work showed that the precipitating solution pH was one of the most important factors affecting the types of precipitates. Therefore, three different precipitating solution pHs were chosen at molar product ($[Ca][ATMP]$) of 0.08 M^2 and calcium to ATMP molar ratio in the systems of 10:1 for the synthesis of three types of Ca-ATMP precipitates. First, batch synthesis experiment was conducted at pH of 1.5, while the second and the third batch were performed at pH of 4 and 7, respectively. All batch synthesis conditions and characterization results were shown in Table 4.1. As the previous work, the complete results were depicted in Figure 4.1.

Table 4.1 Summary of batch synthesis and characterization experiments for Ca-ATMP precipitation.

Precipitating Conditions			Characteristic of Precipitates		
pH	Ca/ATMP Molar ratio	Molar Product [Ca][ATMP] (M^2)	Ca/ATMP Molar ratio	Morphology	Structure
1.5	10:1	0.08	1.04:1	Sheet	Crystalline
4.0	10:1	0.08	2.06:1	Spherical	Amorphous
7.0	10:1	0.08	3.11:1	Spherical	Amorphous

At pH of 1.5, one calcium atom reacted with one active phosphate group in a ATMP molecule resulting in Ca/ATMP molar ratio of 1:1 in the resulting precipitates. At pH of 4, two calcium atoms attached to two active phosphate groups in one ATMP molecule resulting in 2:1 Ca-ATMP molar ratio, while three calcium atoms could bond with three phosphate groups at solution pH of 7, producing the molar ratio of 3:1. The general precipitation reaction of a phosphonate with a divalent cation was shown in Figure 4.2 with calcium and ATMP as the participating co-reactants. The proposed precipitate structure comprising five molecule rings was known to be extremely stable molecular structures (Martell and Calvin, 1956).

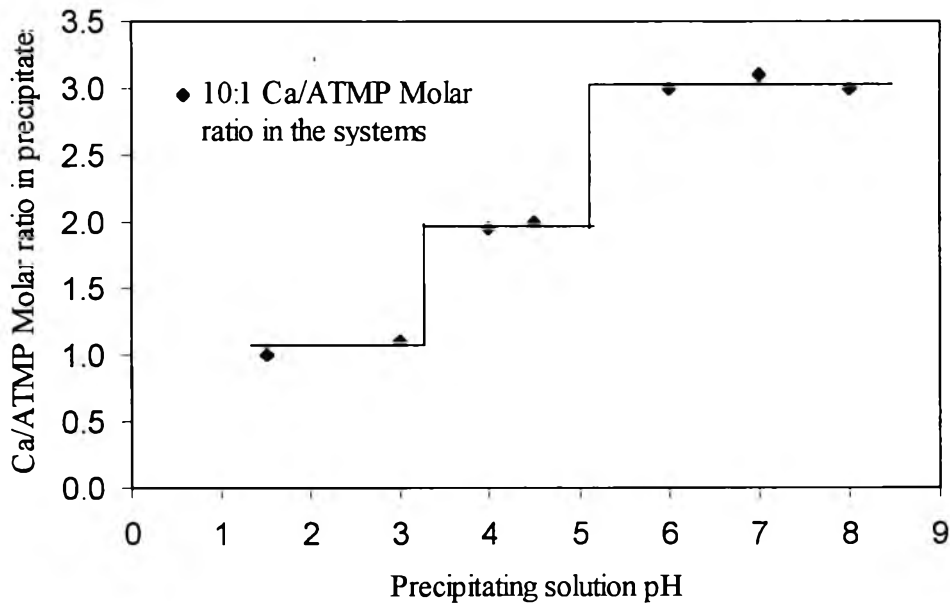


Figure 4.1 Effect of precipitating solution pH on the precipitate compositions (Rerkpattanapipat, 1996).

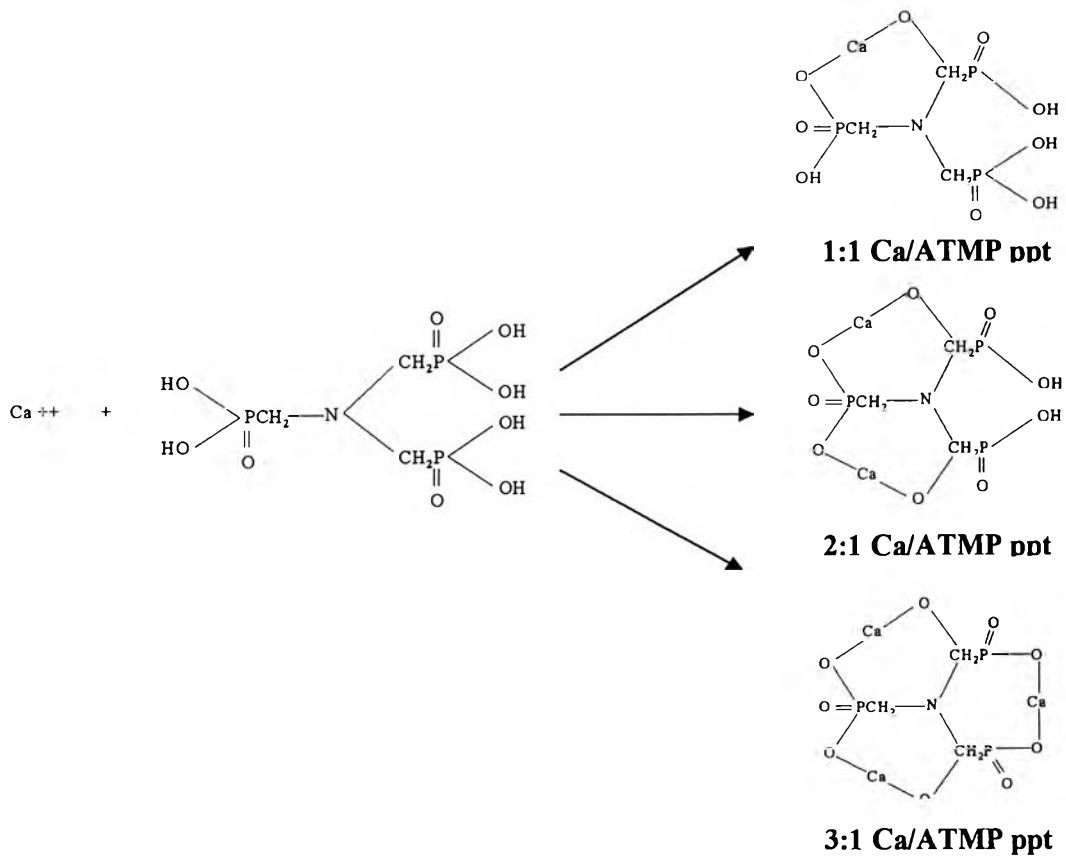


Figure 4.2 Precipitation reaction mechanism between calcium and ATMP.

This phenomenon can be simply described that as the precipitating solution pH increases the solution equilibrium shifts, resulting in increasing the number of hydrogen deprotonated from each ATMP molecule. As a result, calcium ion has more available reacting sites on ATMP molecule at higher pH, resulting in increasing Ca to ATMP molar ratios of precipitates.

A closer examination of Figure 4.1 reveals two interesting phenomena. First, it was obvious that every batch synthesis carried out at constant pH resulted in the formation of one of the three different precipitates (1:1, 2:1 or 3:1) without a presence of the mixture. This indicates that one precipitate was more stable than the others at a given pH value. Second, there were two transition regions where the resulting precipitate's molar ratios was abruptly shifted from 1:1 to 2:1 or 2:1 to 3:1. It was suggested that in this short transition region, a significant change in the system chemistry was occurred. In order to clearly understand these phenomena, the reactions that concerned the formation of each distinct precipitate must be investigated. At a given pH value, the precipitation reaction for 1:1 Ca/ATMP precipitate can be written as



where the equilibrium constant is expressed in terms of activity as

$$K_{eq_1} = \frac{a_{\text{CaATMP}}}{a_{\text{Ca}^{2+}} a_{\text{ATMP}^{2-}}} = \frac{1}{K_{sp_1}} \quad (2)$$

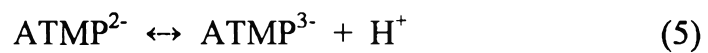
For 2:1 Ca/ATMP precipitate, the ATMP molecule has to deprotonate at least three hydrogen atoms to form a 2:1 precipitate. The precipitation reaction can be written as



while equilibrium constant is defined by the following equation

$$K_{eq_2} = \frac{a_{\text{Ca}_2\text{ATMP}} a_{\text{H}^+}}{a_{\text{Ca}^{2+}}^2 a_{\text{ATMP}^{3-}}} = \frac{1}{K_{sp_2}} \quad (4)$$

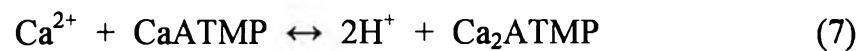
In addition to the two precipitation reactions, the following deprotonation reaction also occurs.



where the equilibrium acid constant is shown as

$$K_a = \frac{a_{\text{ATMP}^{3-}} a_{\text{H}^+}}{a_{\text{ATMP}^{2-}}} \quad (6)$$

By coupling of these equations together, a simple equilibrium expression relating the 1:1 and 2:1 Ca/ATMP precipitate can be written as



An activity of the solid precipitates is assumed to be 1, hence the equilibrium constant can be expressed as

$$K = K_a \frac{K_{eq_2}}{K_{eq_1}} = \frac{a_{\text{H}^+}^2}{a_{\text{Ca}^{2+}}} = K_a \frac{K_{sp_1}}{K_{sp_2}} \quad (8)$$

As an activity is directly related to the concentration, this equation is changed in terms of the molar concentration as shown below.

$$K = K_a \frac{K_{eq2}}{K_{eq1}} = \frac{[H^+]^2}{[Ca^{2+}]} = K_a \frac{K_{sp1}}{K_{sp2}} \quad (9)$$

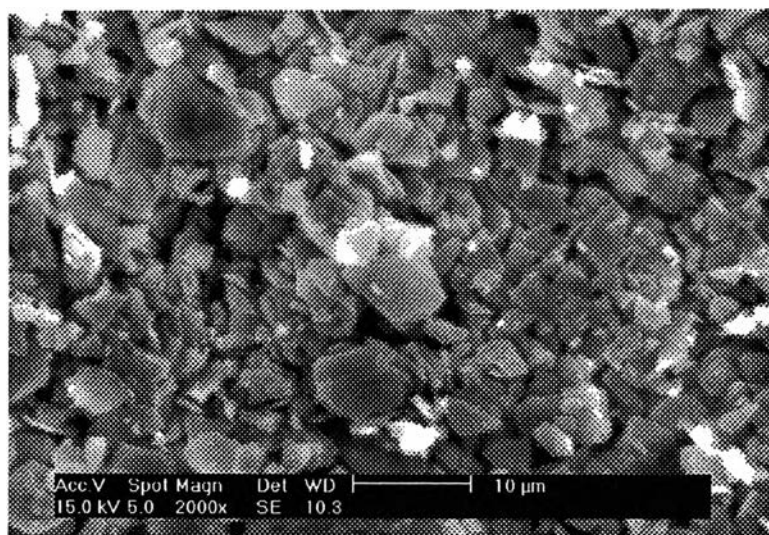
where $[Ca^{2+}]$ is referred to the free calcium cation in the precipitating solution.

From equations (7) and (9), it is obvious that an increase in the calcium concentration or a decrease in the hydrogen concentration (increasing the solution pH) will drive the equilibrium reaction to favor the formation of the 2:1 Ca/ATMP precipitate at the expense of the 1:1 Ca/ATMP precipitate. In addition, equation (9) also reveals that the transition point from a 1:1 to 2:1 Ca/ATMP precipitate occurred when the $[H^+]^2/[Ca^{2+}]$ molar ratio of the precipitating solution was essentially equal to the equilibrium constant (K). The magnitude of this ratio with respect to the equilibrium constant dictates which distinct precipitate was more favorable or which reaction direction is dominant.

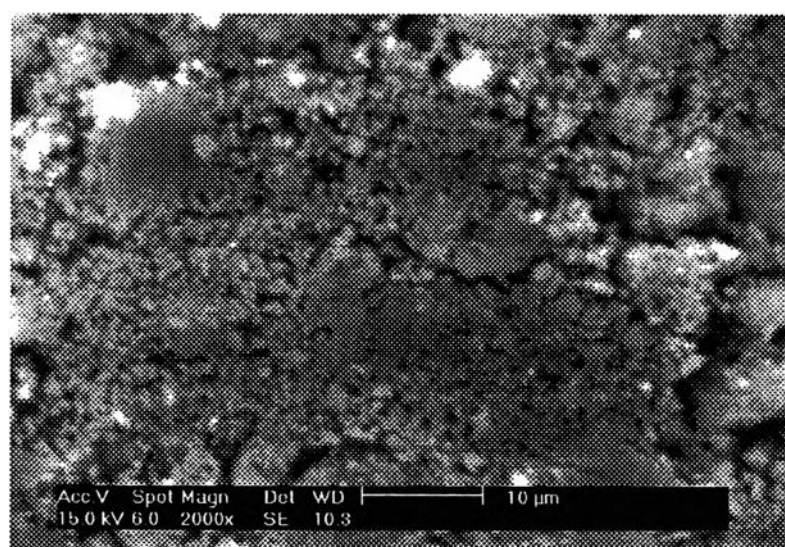
In all batch synthesis experiments, the titration was performed at constant pH, therefore the $[H^+]^2/[Ca^{2+}]$ molar ratio in supernatant relative to the equilibrium constant was also maintain resulting in forming only one distinct precipitate at a given pH value. The transition region from a 2:1 to 3:1 Ca-ATMP precipitate can be also examined in a similar manner as described above.

To confirm the reproducible results, two distinct precipitates, 1:1 and 2:1 Ca/ATMP precipitates were chosen for studying the morphology and structure properties. The morphologies of these two precipitates were studied by using a Scanning Electron Microscope (SEM) as shown in Figure 4.3. It was apparent that the morphologies of 1:1 Ca-ATMP precipitate were sheet particles whereas 2:1 Ca-ATMP precipitate were powdery spherical particles. Figure 4.4 shows the XRD patterns of two precipitates indicating that 1:1

Figure 4.4 shows the XRD patterns of two precipitates indicating that 1:1 Ca/ATMP precipitate has crystalline structure as shown by sharp peaks, while no sharp peaks are observed for 2:1 Ca/ATMP precipitates resulting from its amorphous structure.

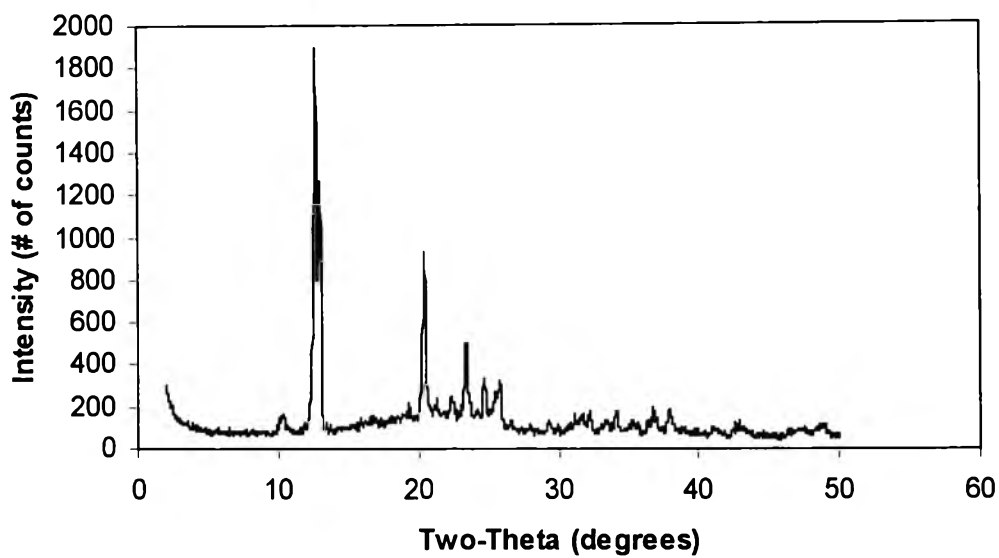


(a) 1:1 Ca/ATMP precipitate synthesized at pH 1.5

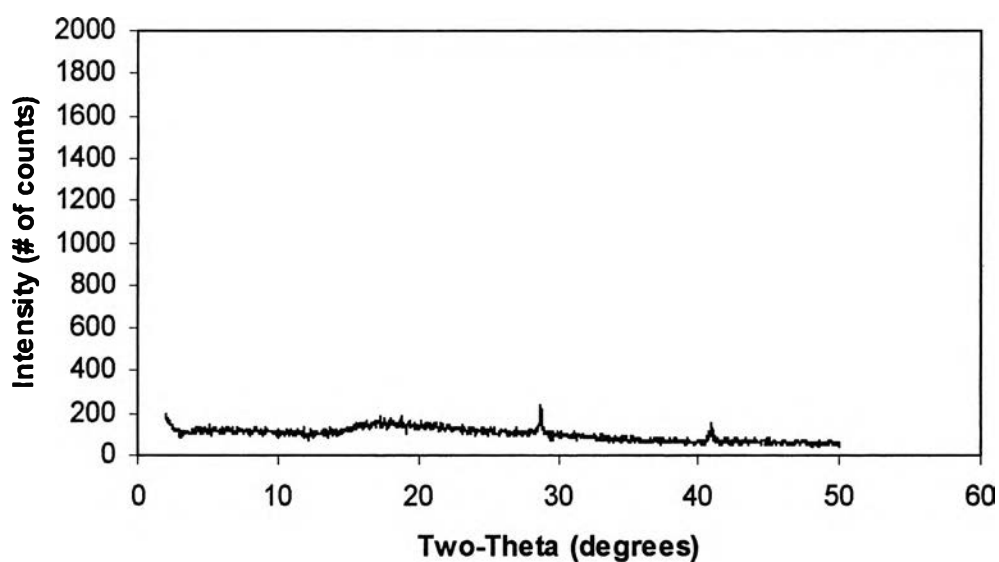


(b) 2:1 Ca/ATMP precipitate synthesized at pH 4

Figure 4.3 Morphological structures of two distinct Ca-ATMP precipitates.



(a) 1:1 Ca/ATMP precipitate synthesized at pH 1.5



(b) 2:1 Ca/ATMP precipitate synthesized at pH 4

Figure 4.4 X-ray diffraction patterns of two distinct Ca-ATMP precipitates.

4.1.2 Mg-ATMP Precipitates

Before the effect of magnesium ion on the Ca-ATMP precipitation was studied, the precipitation between magnesium and ATMP was performed first in order to examine the precipitation performance of magnesium ion with ATMP molecule. The method for forming Mg-ATMP precipitates was mentioned in the experimental section. Table 4.2 shows the precipitating conditions and characterization of the resulting Mg-ATMP precipitates, where the precipitating solution pHs (1.5, 4 and 7) and Mg/ATMP molar ratio in the systems (10:1) were similar to the Ca-ATMP precipitation.

Table 4.2 Summary of batch synthesis and characterization experiments for Mg-ATMP precipitation.

Precipitating Conditions			Characteristic of Precipitates		
pH	Mg/ATMP Molar ratio	Molar Product ([Mg][ATMP]) (M ²)	Mg/ATMP Molar ratio	Morphology	Structure
1.5	10:1	0.85	1.19:1	Sheet	Crystalline
1.5	10:1	0.80	1.10:1	Sheet	Crystalline
4.0	10:1	0.10	XXXX	****	****
4.0	10:1	0.08	XXXX	****	****
7.0	10:1	0.08	XXXX	****	****
7.0	10:1	0.05	XXXX	****	****

XXXX and **** No precipitate formed and no analysis , respectively.

At the solution pH of 1.5, it was found that the approximate 1:1 Mg/ATMP molar ratio in the resulting precipitate can only be formed at the

molar product of 0.80 M^2 or higher, while the molar product of 0.08 M^2 was enough for synthesizing 1:1 Ca/ATMP precipitate. As a molar product relates to a solubility product (K_{sp}) of precipitates as defined in equation (10), it is apparent that 1:1 Mg/ATMP precipitate had higher solubility product than 1:1 Ca-ATMP precipitate at the same pH value. This solubility product is a thermodynamics property which depends upon the types of precipitates. A solubility product of 1:1 Mg/ATMP precipitate was expressed as

$$K_{sp} = [\text{Mg}^{2+}][\text{ATMP}^{2-}] \quad (10)$$

At the solution pHs of 4 and 7, no precipitates were observed at those molar product values. In order to form precipitates, the molar products were necessary to overcome the solubility product. Unfortunately, the molar products at pH 4 and 7 could not be really increased more than those values because magnesium hydroxide was apparently formed in the systems, as well as having strong effect on controlling the precipitating solution pH during the titration.

The morphology of 1:1 Mg/ATMP precipitate is illustrated in Figure 4.5 indicating many sheet particles similar to the morphology of 1:1 Ca/ATMP precipitate. The X-ray diffraction pattern of this precipitate shown in Figure 4.6 clearly confirms that it is crystalline in nature.

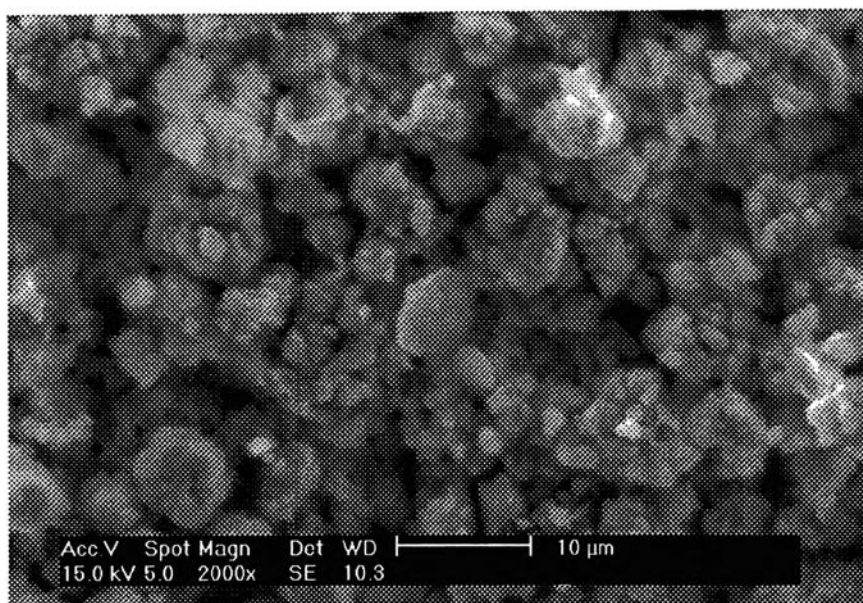


Figure 4.5 Morphological structure of the precipitate having 1:1 Mg/ATMP molar ratio.

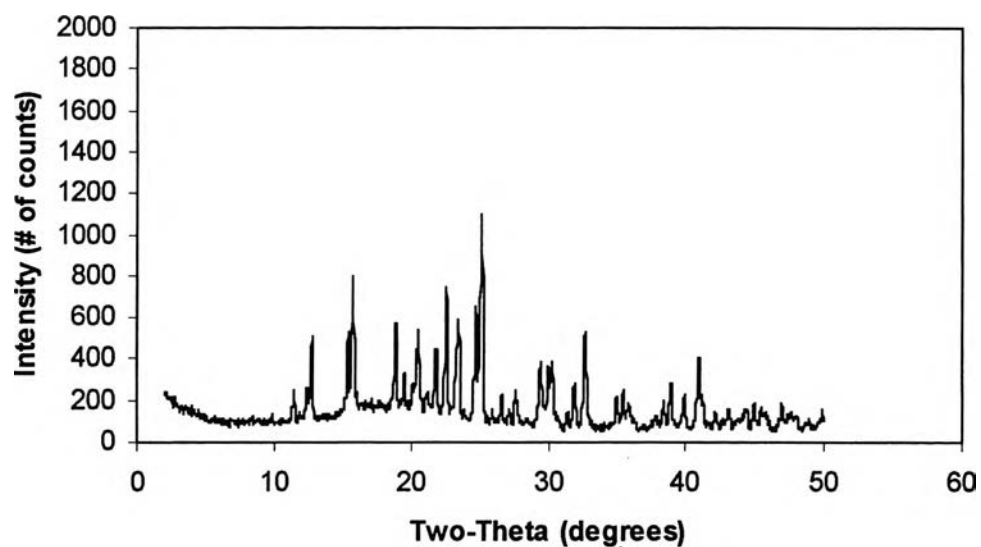


Figure 4.6 X-ray diffraction pattern of 1:1 Mg/ATMP precipitate formed at precipitating solution pH of 1.5 and molar product of 0.80 M².

4.1.3 Ca-ATMP Precipitates with the Presence of Magnesium Ion

This part was conducted based on the fact that in addition to the presence of calcium ion in the formation water, it also has a large amount of magnesium ion, which could be able to precipitate with phosphonate as well. The methodology was also the same as Ca-ATMP precipitation synthesis except that magnesium and ATMP solution were combined together before being titrated with calcium solution. When magnesium solution was introduced into ATMP solution, the solution pH decreased rapidly because of the chelation chemistry and no Mg-ATMP precipitate was observed. The molar product of $[Ca][ATMP]$ was kept constant at 0.08 M^2 , while three precipitating solution pHs were 1.5, 4 and 7. The effect of magnesium ion was directly examined by varying magnesium concentration in terms of total calcium to magnesium molar ratios in the system of 0.5:1, 1:1, 2:1 and 5:1. All batch synthesis conditions and characterization results are shown in Table 4.3.

A closer evaluation of this table revealed several interesting phenomena. First, from Figure 4.7, a small amount of magnesium ion found in the resulting precipitate was observed during varying the total Ca/Mg molar ratio in the systems from 1:1 to 5:1 (total magnesium concentration added into the systems) at precipitating solution pH of 1.5. In addition, the Ca/ATMP molar ratios in the resulting precipitates were approximately constant at 1:1. It was indicated that magnesium ion had little effect on the Ca-ATMP precipitates or no interaction between magnesium ion and ATMP molecules at this precipitating solution pH, or in other words only Ca-ATMP precipitate approximately had Ca/Mg molar ratio of 1:1 was formed. The explanation was offered in terms of the solubility product related to the molar product used.

In order to form 1:1 Mg/ATMP precipitate, the molar product should be at least 0.8 M^2 or higher (see Table 4.2). However, by varying the total Ca/Mg molar ratio from 5:1 to 1:1, the maximum molar product for

Table 4.3 Summary of different batch synthesis condition and characterization of resulting precipitates with the presence of magnesium ion.

Conditions of Precipitating Solution					Precipitate Characteristics					
No	pH	Total Ca/Mg Molar Ratio	Ionic str. (Approx.) (M)	[Mg][ATMP] Molar Product (M ²)	Ca/ATMP Molar Ratio	Mg/ATMP Molar Ratio	Total molar ratio Ca+Mg/ATMP	Ca/Mg Molar Ratio	Precipitate Morphology	Precipitate Structure
1	1.5	0.5:1	8.05	0.160	1.21:1	0.90:1	2.11:1	*****	Spherical Particles	Amorphous
2	1.5	1:1	5.37	0.080	1.04:1	No Mg present	1.04:1	*****	Sheet Particles	Crystalline
3	1.5	2:1	4.03	0.040	1.09:1	No Mg present	1.09:1	*****	*****	*****
4	1.5	5:1	3.22	0.016	1.12:1	No Mg present	1.12:1	*****	*****	*****
5	4.0	0.5:1	8.05	0.160	xxxxx	xxxxx	xxxxx	*****	*****	*****
6	4.0	1:1	5.37	0.080	1.33:1	1.04:1	2.37:1	1.35:1	Spherical Particles	Amorphous
7	4.0	2:1	4.03	0.040	1.54:1	0.70:1	2.24:1	2.31:1	*****	*****
8	4.0	5:1	3.22	0.016	1.78:1	0.40:1	2.18:1	4.62:1	*****	*****
9	7.0	0.5:1	8.05	0.160	1.28:1	1.80:1	3.07:1	0.78:1	*****	*****
10	7.0	1:1	5.37	0.080	1.89:1	1.41:1	3.29:1	1.21:1	Spherical Particles	Amorphous
11	7.0	2:1	4.03	0.040	2.19:1	0.93:1	3.12:1	2.23:1	*****	*****
12	7.0	5:1	3.22	0.016	2.44:1	0.57:1	3.01:1	4.44:1	*****	*****

[Ca][ATMP] molar product and [Ca]/[ATMP] molar ratio in the systems were constant at 0.08 M² and 10:1, respectively

xxxxx No precipitates formed at this condition

***** No Analysis at this condition

$[Mg][ATMP]$ was only $0.08 M^2$ (see Table 4.3) that was not enough to overcome the solubility product resulting in no 1:1 Mg/ATMP precipitate.

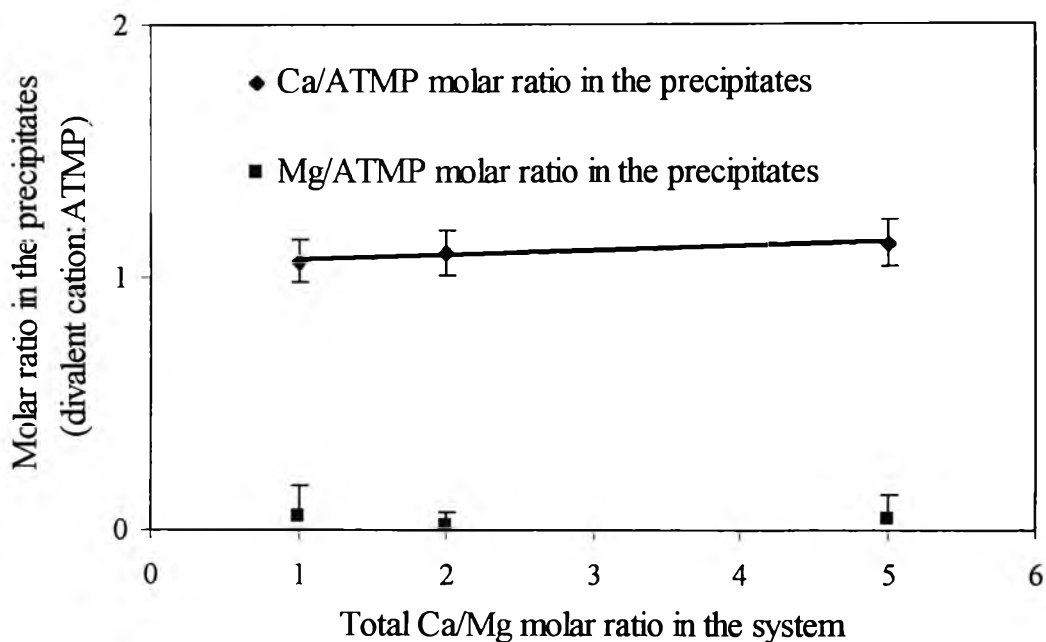


Figure 4.7 Effect of total Mg added in the system on the compositions of the precipitates formed at precipitating solution pH of 1.5.

One of these resulting precipitates formed in the solution having pH of 1.5 and the total Ca/Mg molar ratio of 1:1 was selected to study the morphology property as shown in Figure 4.8, illustrating sheet particles. In Figure 4.9, the XRD pattern of this precipitate clearly confirmed that it was composed of only 1:1 Ca/ATMP precipitate because the pattern of crystalline structure was the same as that of 1:1 Ca/ATMP precipitate synthesized from the system without the presence of Mg.

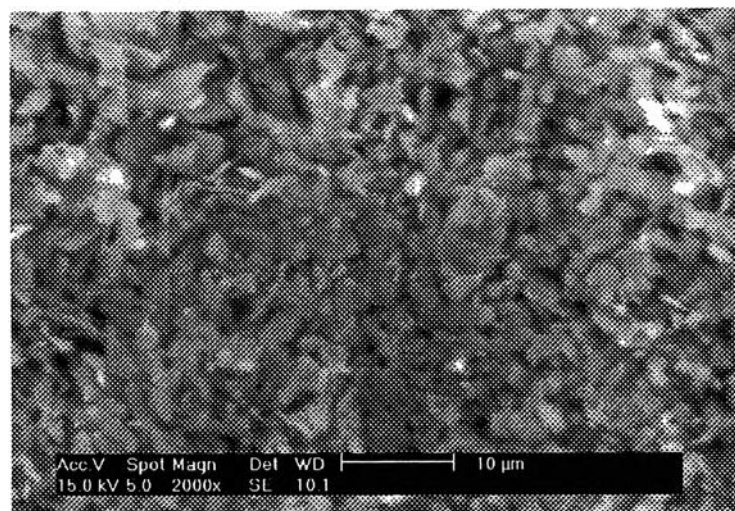


Figure 4.8 Morphological structure of the precipitate having total molar ratio of 1:1 formed at precipitating solution pH of 1.5 and total Ca/Mg molar ratio in the system = 1:1.

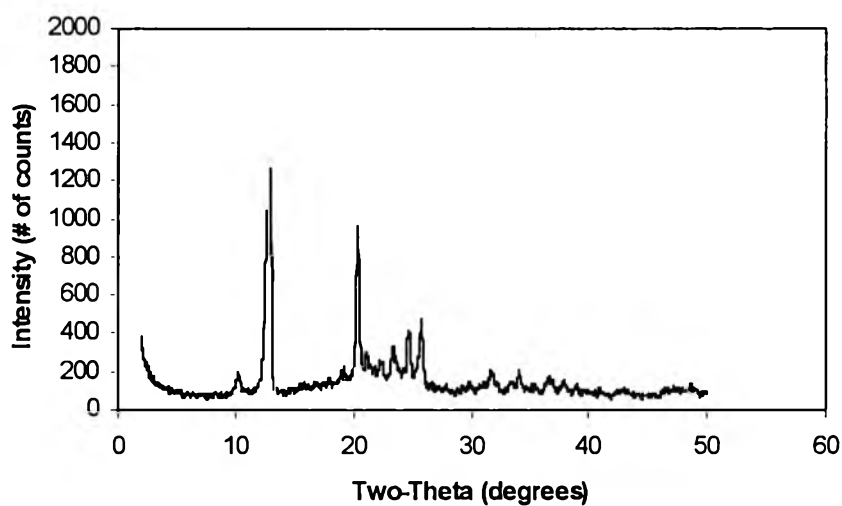


Figure 4.9 X-ray diffraction pattern of the precipitate having total molar ratio of 1:1 formed at precipitating solution pH of 1.5 and total Ca/Mg molar ratio in the system = 1:1.

Second, significant amount of magnesium ion was detected in the resulting precipitates formed at precipitating solution pH of 4. As can be seen in Figure 4.10, Ca/ATMP molar ratio in the precipitates decreased with decreasing total Ca/Mg molar ratio or increasing total magnesium concentration added into the systems, while Mg/ATMP molar ratio in the precipitate increases. These observations imply that some of the reacting sites on ATMP molecules were reacted with magnesium ions instead of calcium ions resulting in a decrease of Ca/ATMP molar ratio in the precipitate. However, the total molar ratio in the precipitate defined as the summation of calcium and magnesium concentration found in the precipitates divided by ATMP concentration were constant at approximate 2:1 indicating that the precipitates containing two divalent cations and one ATMP molecule were the most stable structure for the precipitates formed at this solution pH.

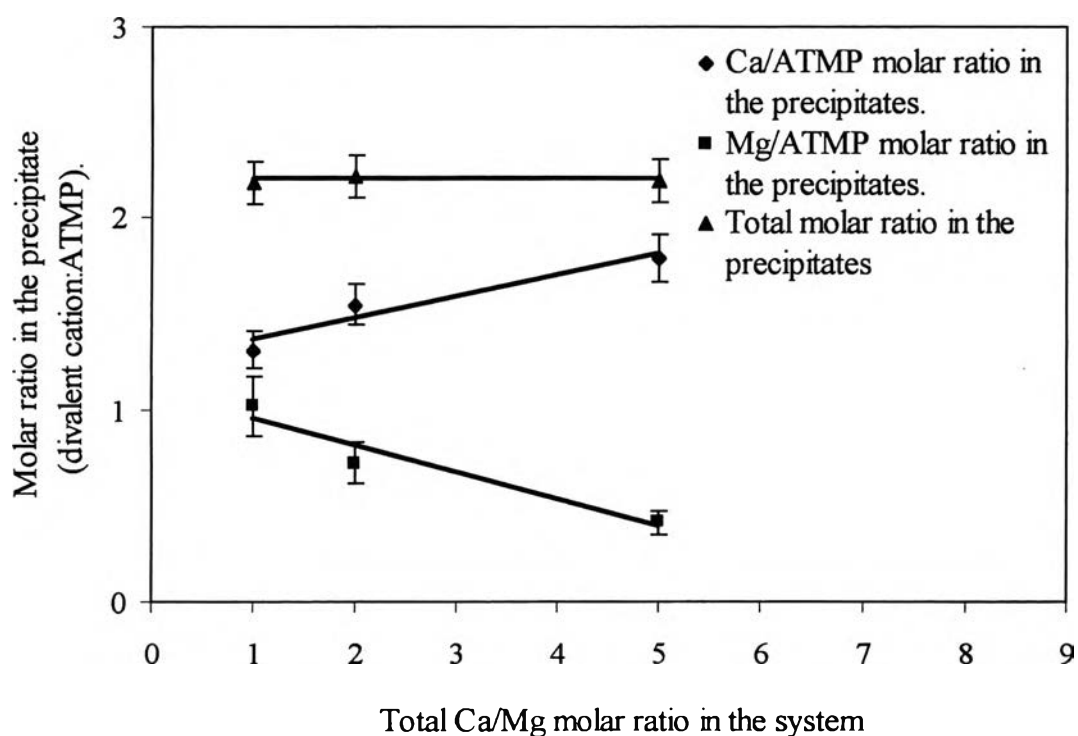


Figure 4.10 Effect of total Mg added in the system on the compositions of the precipitates formed at precipitating solution pH of 4.

The same phenomena were also observed from the resulting precipitates formed at precipitating solution pH of 7 during varying the total Ca/Mg molar ratio in the systems from 0.5:1 to 5:1 as shown in Figure 4.11. Moreover, the most stable structure of the precipitates formed at this pH composed of three divalent cations bonding with one ATMP molecule resulting in the precipitate's total molar ratio of 3:1.

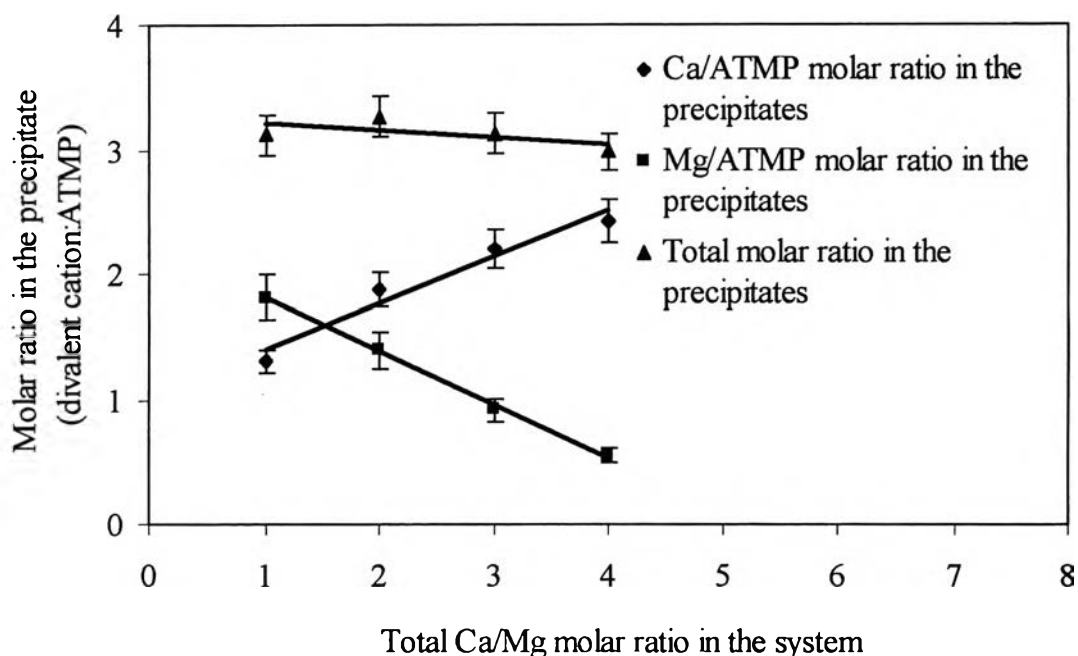


Figure 4.11 Effect of total Mg added in the system on the compositions of the precipitate formed at precipitating solution pH of 7.

Figure 4.12 demonstrates the effect of total magnesium concentration added into the system on the magnesium content in the resulting precipitates formed at precipitating solution pH of 4 and 7. It was found that a decrease in the total Ca/Mg molar ratio or increase in the total magnesium concentration in the system resulted in an increase in magnesium content in the resulting precipitate. Interestingly, there was no significant effect of the solution pH in the studied range on the correlation between the total Ca/Mg molar ratio in the system and the Ca/Mg molar ratio in the resulting precipitate.

Moreover, the Ca/Mg molar ratio in the resulting precipitate increased almost linearly with increasing the total Ca/Mg molar ratio in the system.

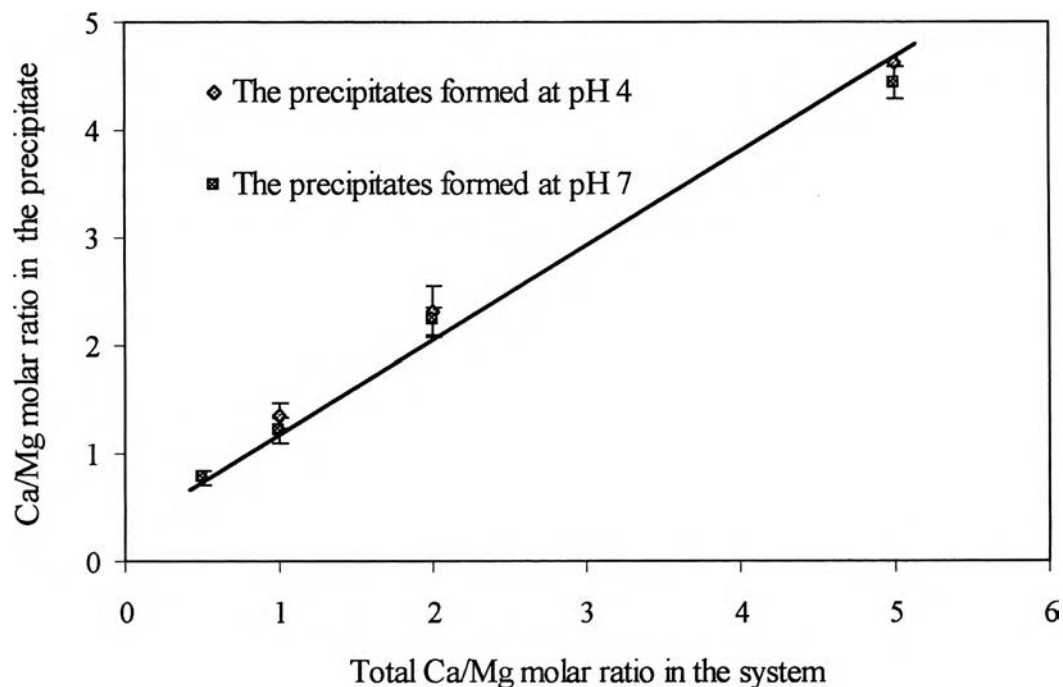


Figure 4.12 Effect of total Mg concentration added in the system on the Mg content in the precipitate.

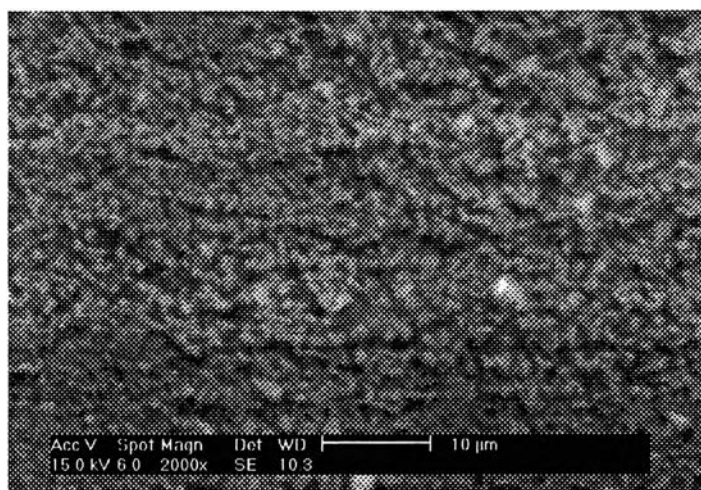
It can be simply described by equilibrium equation as expressed in equation (11).



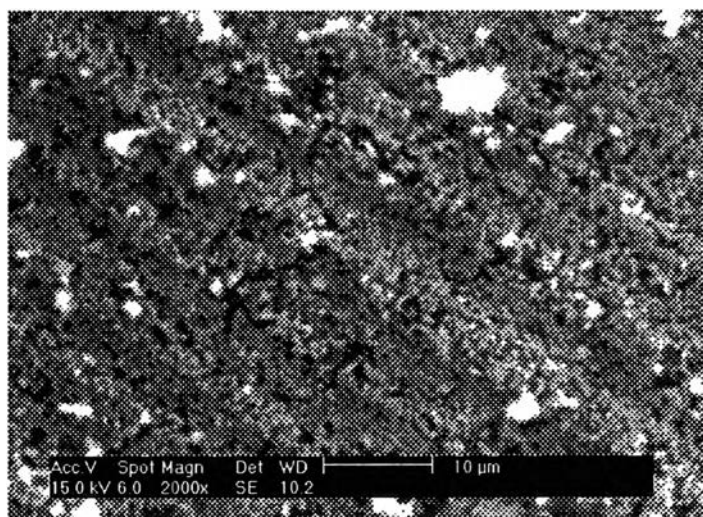
As the concentration of magnesium increases, the equilibrium reaction is shifted to the right hand side of the reaction equation following Le Chalelier Principle. As a result, a higher total concentration of magnesium in the system, the higher amount of magnesium content in the resulting precipitate was obtained while a decrease in the Ca/ATMP molar ratio of this resulting precipitate was observed. This observation implies that magnesium ion could potentially compete with calcium ion for the precipitate formation.

Both resulting precipitates containing both calcium and magnesium ions and having approximately total molar ratios of 2:1 and 3:1

synthesized under the precipitating solution pHs of 4 and 7 were chosen to study their morphology and structure. As can be seen from Figure 4.13 and 4.14, these two precipitates look the same like spherical particles, while the XRD patterns demonstrate amorphous structure in nature which were also similar to the properties of 2:1 and 3:1 Ca/ATMP precipitates.

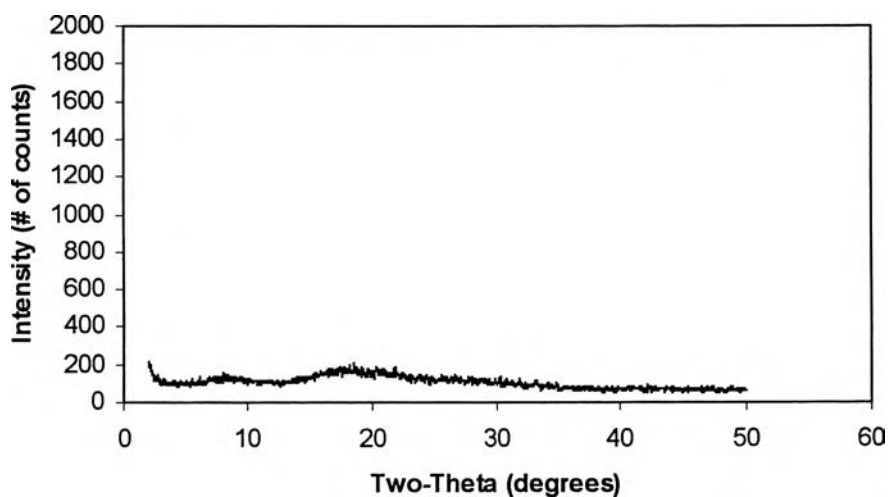


(a) The resulting precipitate having the total molar ratio of 2:1 synthesized from batch 6 in Table 4.3

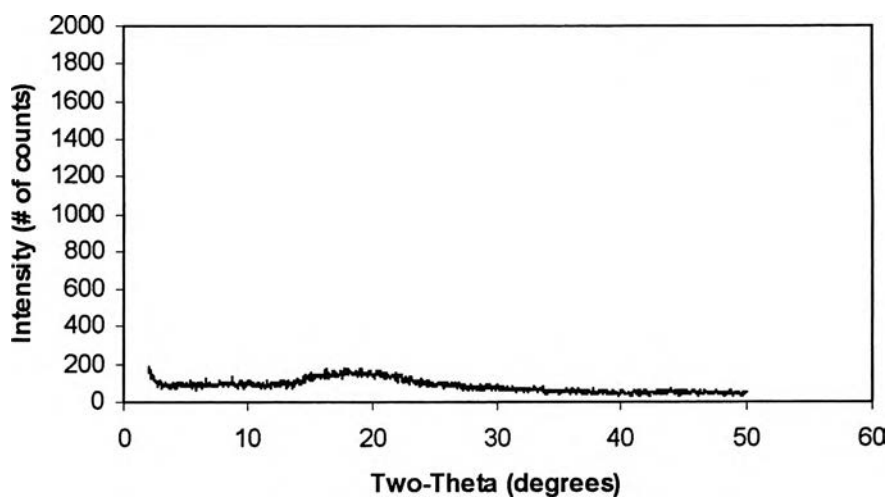


(b) The resulting precipitate having the total molar ratio of 3:1 synthesized from batch 10 in Table 4.3

Figure 4.13 Morphological structures of two different total molar ratios of the resulting precipitates.



(a) X-ray diffraction pattern of the resulting precipitate having the total molar ratio of 2:1 synthesized from batch 6 in Table 4.3.



(b) X-ray diffraction pattern of the resulting precipitate having the total molar ratio of 3:1 synthesized from batch 10 in Table 4.3.

Figure 4.14 X-ray diffraction patterns of two different total molar ratios of the resulting precipitates.

4.1.4 Proposed Mechanism of Precipitates formed between ATMP and Calcium with Magnesium

Since the magnesium content was found in the precipitates formed at the precipitating solution pHs of 4 and 7, it was necessary to identify a formation structure of magnesium ion with ATMP molecule. Two possible mechanisms for the precipitate formation with magnesium and calcium ions proposed are co-precipitation and complex precipitation.

4.1.4.1 Co-Precipitation

Since phosphonate scale inhibitors can interact with any divalent cations resulting in the formation of precipitates, magnesium ion may be also able to form precipitates with phosphonate scale inhibitors. Therefore, a precipitate formed in this system appear as a mixture of different divalent cations-scale inhibitor precipitates (e.g., Ca-ATMP precipitate + Mg-ATMP precipitate). Based on the total molar ratios and Ca/Mg molar ratios in the resulting precipitate, the simple precipitate structure is proposed as shown in Figure 4.15.

4.1.4.2 Complex Precipitation

This system is proposed based on the fact that ATMP as a phosphonate scale inhibitor has three numbers of active phosphate groups for binding with divalent cations. It may have the competition between different divalent cations with active phosphate groups. Figure 4.16 shows the possible structures of the precipitates formed at both pH values by complex precipitation.

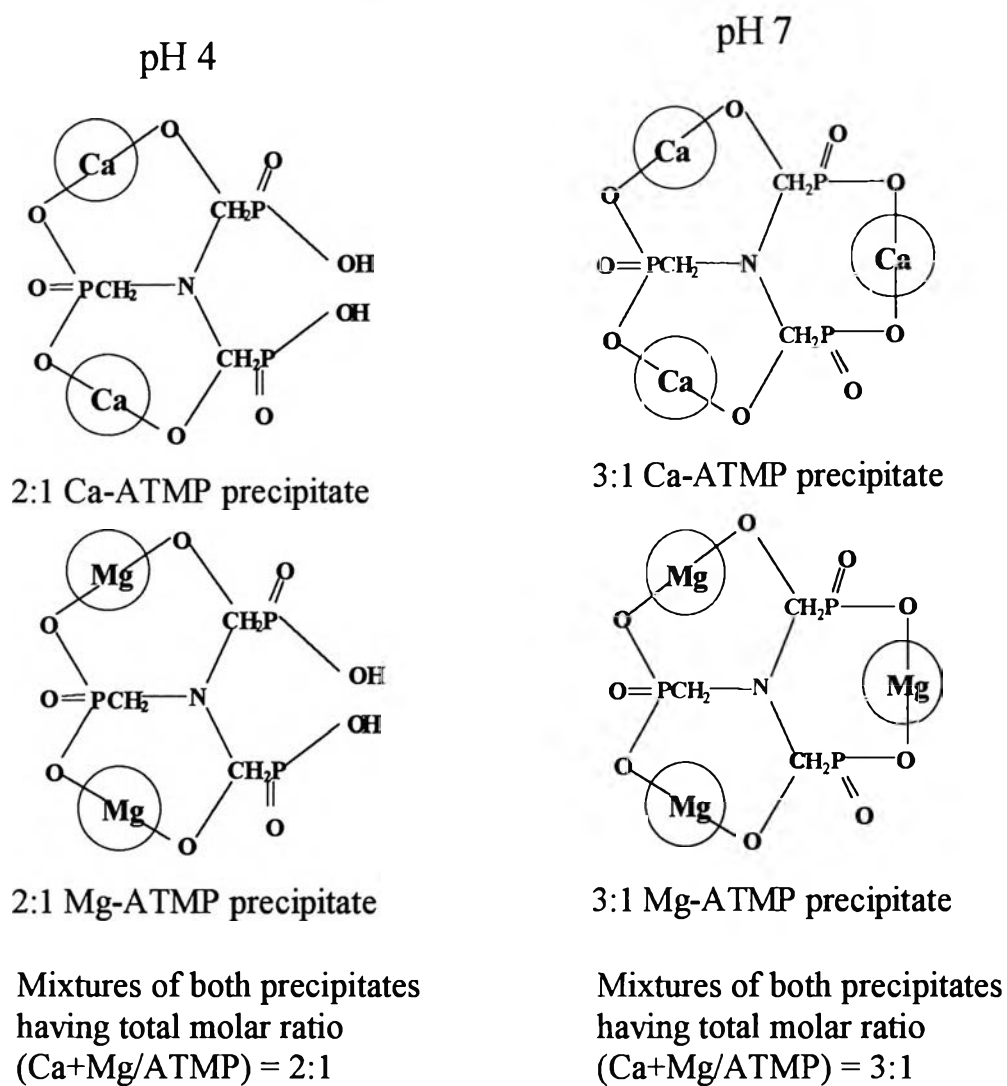


Figure 4.15 Possible structures for precipitate formation of ATMP with Ca and Mg ions by co-precipitation.

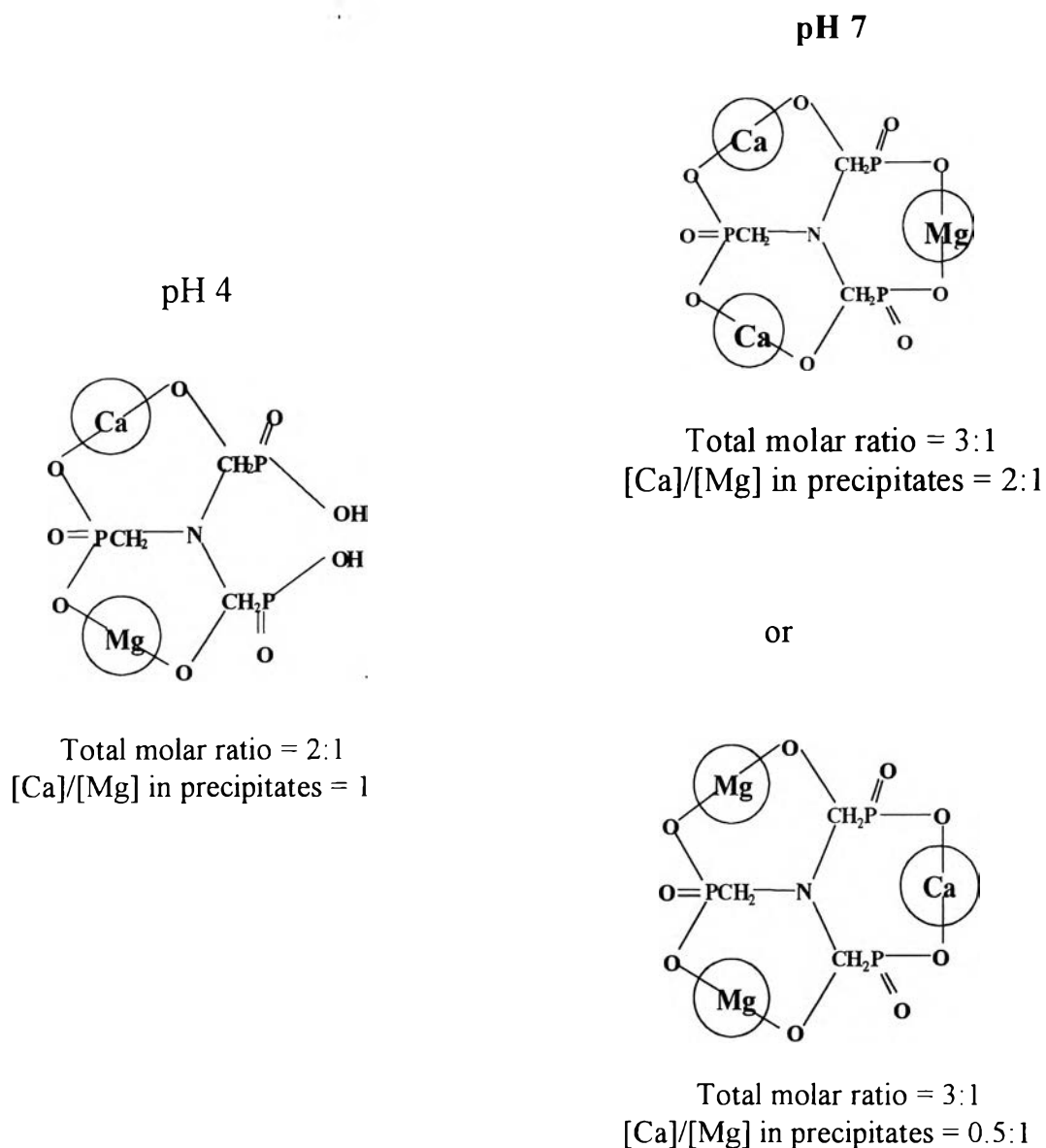


Figure 4.16 Possible structures of precipitate formation of ATMP with Ca and Mg ions by complex precipitation.

It is very interesting to find out whether co-precipitation or complex precipitation is more likely to occur. From Figure 4.16, each atom of calcium and magnesium are bonded with the same ATMP molecule at pH 4 resulting in Ca/Mg molar ratio of 1:1 in precipitate. At pH 7, two atoms of calcium and one atom of magnesium or in the other hand, two atoms of

magnesium and one atom of calcium are reacted with one ATMP molecule producing the Ca/Mg molar ratio of 2:1 or 0.5:1, respectively. If this complex precipitation is valid, these Ca/Mg molar ratios in these two precipitates should not depend upon the total Ca/Mg molar ratio in the system. However, from the results shown in Figure 4.12, it was obvious that the Ca/Mg molar ratio in the resulting precipitate had a linear relationship with total Ca/Mg molar ratio in the system at both solution pHs of 4 and 7. Therefore, it possibly implied that Mg-ATMP precipitates may be able to co-precipitate along with the formation of Ca-ATMP precipitate or in other words, it had the competitive precipitation to each other. This hypothesis was also supported by the results of the batch dissolution study which will be discussed later.

4.1.5 Effect of Ionic Strength on Mg-ATMP Precipitates

It was surprising that in the presence of calcium, Mg-ATMP precipitate could be formed which in the absence of calcium, it could not be formed as mention in the results of the batch synthesis of Mg-ATMP precipitates. These might be due to the effect of introducing calcium ion which results in an increase in ionic strength. In order to investigate the effect of ionic strength, sodium chloride solution was used instead of calcium solution for the titration because sodium ions cannot react with phosphonate molecules due to monovalent cations. The amount of sodium chloride used was calculated in order to maintain the same ionic strength as shown in Table 4.3. The experimental method was the same as described in Ca-ATMP precipitation with magnesium ion except that the solution composed of magnesium chloride and ATMP was titrated with sodium chloride solution.

Table 4.4 shows the results of the experiment conducted at the same ionic strength and three values of precipitating solution pH (as the same as in Table 4.3). At the solution pH of 1.5, no Mg-ATMP precipitate was observed, while 2:1Mg/ATMP precipitate and 3:1 Mg/ATMP precipitates were formed at

terms of equilibrium acid constant (K'_a) relating to the formation of Mg-ATMP precipitates.

Table 4.4 Summary of batch synthesis of Mg-ATMP precipitates in the presence of NaCl.

Precipitating Conditions				Mg/ATMP Molar ratio in precipitate
pH	Ionic strength (Approximate) (M)	Molar Product of [Mg][ATMP] (M ²)	Mg/ATMP Molar ratio	
1.5	5.37	0.08	10:1	xxxxx
4	5.37	0.08	10:1	2.29:1
7	5.37	0.08	10:1	3.04:1

xxxxx No precipitates formed

For forming 2:1 precipitate, ATMP has to be deprotonated four hydrogen atoms as



where the equilibrium acid constant is written as

$$K'_a = \frac{[\text{ATMP}^{4-}][\text{H}^+]}{[\text{ATMP}^{3-}]} \quad (13)$$

Taking logarithm both sides, equation (13) becomes as

$$-\log K'_a = -\log[H^+] - \log \frac{[ATMP^{4-}]}{[ATMP^{3-}]} \quad (14)$$

or

$$pK'_a = pH - \log \frac{[ATMP^{4-}]}{[ATMP^{3-}]} \quad (15)$$

and the solubility product for 2:1 Mg-ATMP precipitate can be written as

$$K_{sp} = [Mg^{2+}]^2 [ATMP^{4-}] \quad (16)$$

From previous works (Browning and Fogler, 1993, 1995, 1996 and Rerkpattanapipat, 1996), it was found that equilibrium acid constant (pK'_a) significantly decreased with increasing the ionic strength. As the ionic strength decreases, the phosphonate acid can deprotonate much more hydrogen atoms and results in more conjugated base as well. Because the precipitating solution pH was controlled at a constant value, base on equation (15), the concentration of $ATMP^{4-}$ species apparently increased with a decrease of pK'_a value. Hence, the driving force to overcome K_{sp} is also increased contributing the formation of 2:1 Mg/ATMP precipitate. However, the resulting precipitates cannot be able to precipitate if this increased driving force does not exceed or equals the solubility product.

The last interesting phenomena is the effect of the ionic strength on the total molar ratio of the precipitate as depicted in Figure 4.17. The ionic strength was increased by increasing the total magnesium concentration added into the system which resulted in decreasing the total Ca/Mg molar ratio.. The results showed that the total molar ratio (Ca+Mg:ATMP) of the resulting precipitates formed at precipitating solution pH of 1.5 shifted from 1:1 to 2:1 with substantial increase in the ionic strength from approximately 5.3 to 8.0 M.

The results can be explained by the deprotonation curves of ATMP. The deprotonation curves represent the fraction of deprotonated species at different pH values and they are formulated by calculating from the equilibrium acid constant of phosphonates. Figure 4.18 illustrates the deprotonation curves of ATMP without and with the effect of ionic strength.

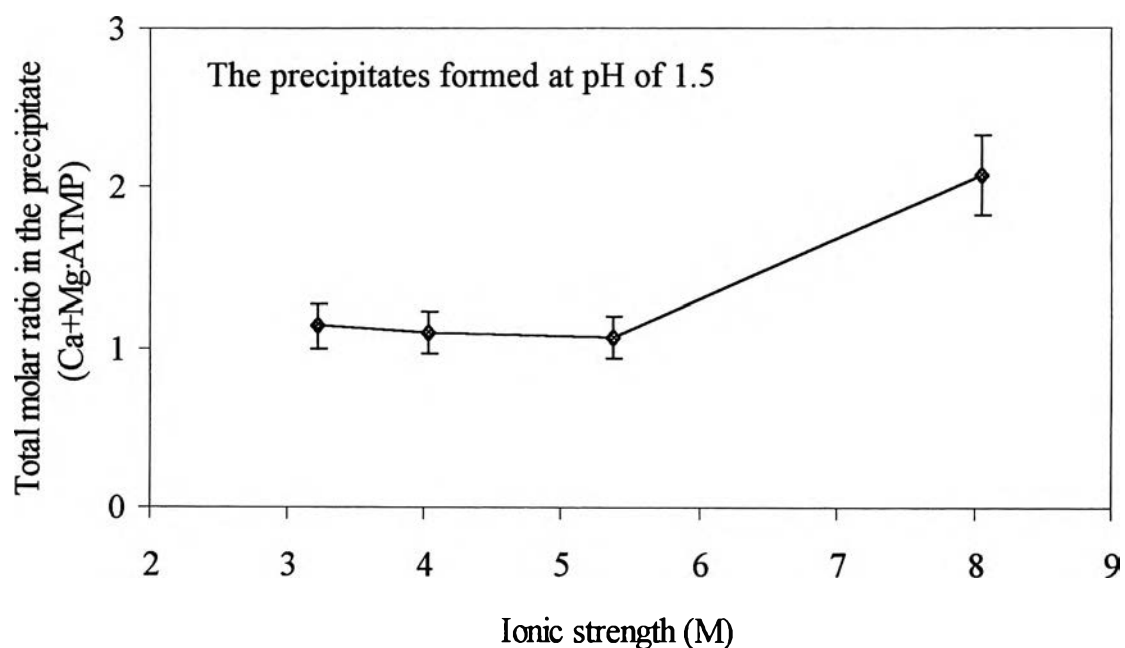
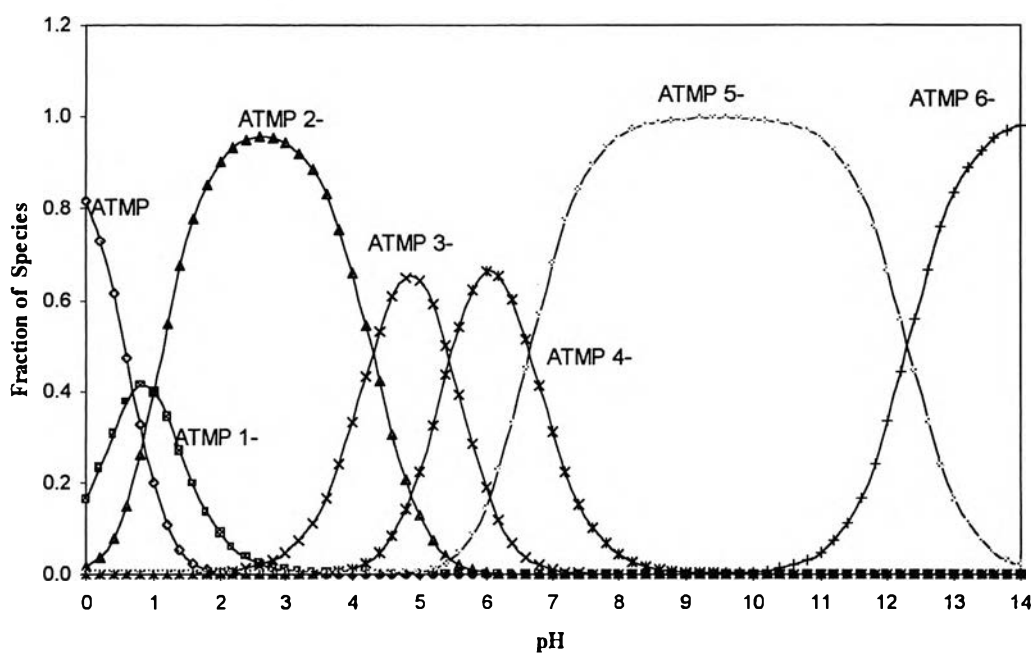


Figure 4.17 Effect of ionic strength on the total molar ratios of the precipitates.

(a) Ionic strength = 0 M



(b) Ionic strength = 0.6 M

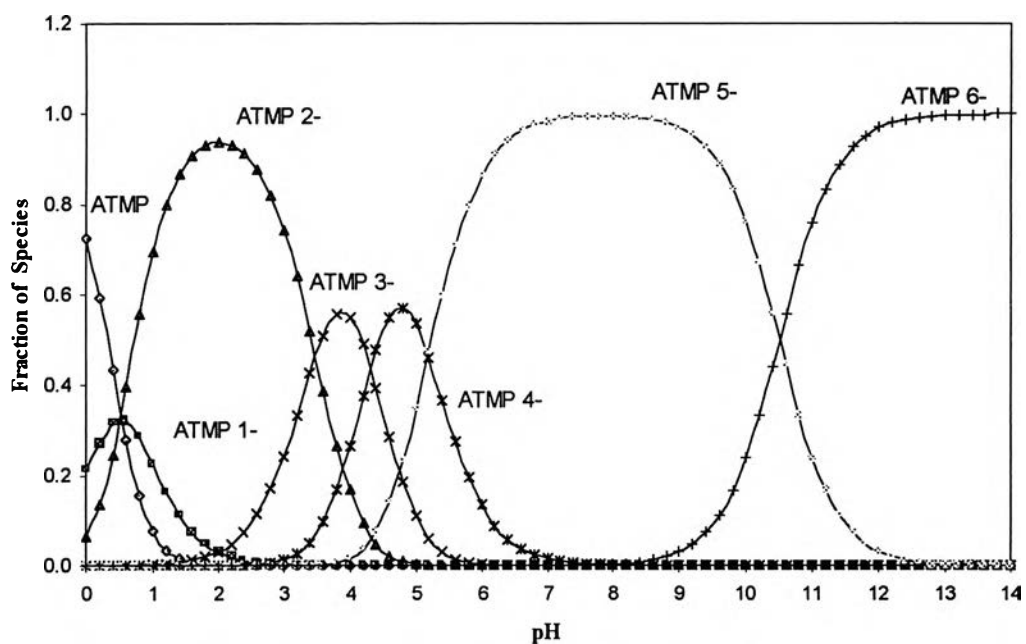


Figure 4.18 The deprotonation curves of ATMP and the resulting species composition without and with the effect of ionic strength.

In order to examine the effect of ionic strength on the deprotonation curves, an approximate form of Debye-Huckel equation (Perrin, 1974) was also taken to account in the calculations as shown in Appendix A. This equation is expressed in the equation below:

$$-\log f_i = \frac{AZ^2I^{0.5}}{(1+I^{0.5})} - 0.1Z^2I \quad (\text{only dilute solution}) \quad (17)$$

where f_i = activity coefficient [-]
 I = ionic strength [M]
 A = a constant which depends on the temperature
 (at 25°C, $A = 0.512$)
 Z = charge

and the ionic strength (I) is given by the summation as

$$I = \frac{1}{2} \sum (C_i Z_i^2) \quad (18)$$

where C_i = the concentration of each types of ion (M)
 Z_i = charge of ions

By considering the deprotonation curves with the effect of ionic strength of approximate 0.6 M (see Figure 4.16 (b)), the whole curves are being shifted to the left hand side compared with no effect of ionic strength as shown in Figure 4.18 (a).

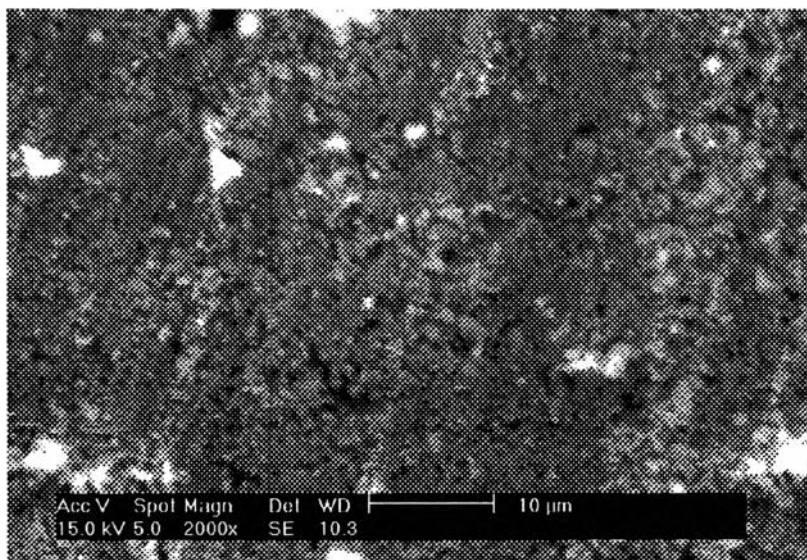
As the deprotonation curves are shifted, the deprotonated species with the higher charge is dominant or in other words the ATMP molecules can

deprotonate much more hydrogen atoms resulting in an increase of precipitate's total molar ratio(Ca+Mg:ATMP). In this case, after substantial shifting in the deprotonation curves, the ATMP^{4-} species was dominant instead of ATMP^{2-} species at the same pH value causing the favorable formation of the 2:1 precipitate.

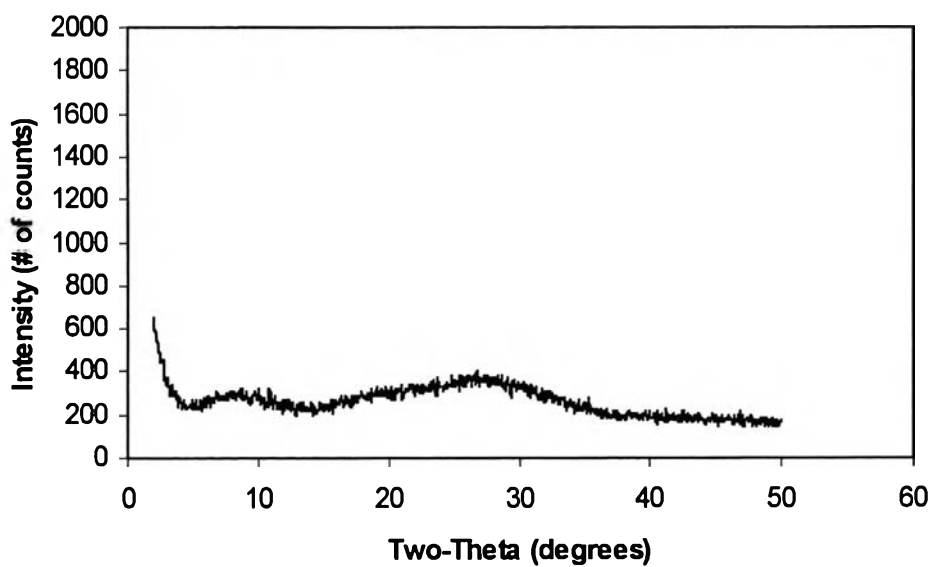
Based on Debye-Huckel equation, the ionic strength cannot be increased more than approximately 0.6 M due to a limitation of this equation (only dilute solution). However, the use of Debye-Huckel equation is good enough to demonstrate the effect of ionic strength on the deprotonation curves.

The complete change of precipitate properties was also confirmed by the morphology and XRD studies which indicate powdery spherical particles and amorphous structure as depicted in Figure 4.19.

However, if the shifted deprotonation curve resulted in more unstable phosphonate species, the precipitates could not be formed. This phenomenon also occurred in Table 4.3, whereas the precipitating solution pH and total Ca/Mg molar ratio were 4 and 0.5, respectively. It was expected that ATMP^{5-} was the most of dominant unstable species occurred at this condition resulting in no precipitate formation (compared with No 6, 7 and 8 in Table 4.3).



(a)



(b)

Figure 4.19 Morphological structure (a) and X-ray diffraction pattern (b) of the resulting precipitate having total molar ratio of 2:1 formed at pH 1.5 and total Ca/Mg molar ratio of 0.5:1 or ionic strength of 8.05 M.

4.2 Dissolution Rates of Precipitates

In order to scientifically prove the mechanism of precipitate formation, batch dissolution experiments of the resulting precipitates were examined by using a rotating disk reactor. An initial dissolution rate was used to represent the dissolution performance of each resulting precipitate and it could be determined from the slope of the graph plotting between concentration and time. To minimize the effect of surface area on the initial rate of dissolution, the resulting precipitates were reformed from powder to pellets having the same surface area of 3 cm^2 by using a hydraulic press. The batch dissolution experiments were classified into three main parts, dissolution of Ca-ATMP precipitates, Mg-ATMP precipitates and mixed precipitates.

4.2.1 Dissolution Rates of Ca-ATMP Precipitates

The dissolution rates of three distinct precipitates formed at precipitating solution pHs of 1.5, 4 and 7 are determined experimentally as shown in Figure 4.20.

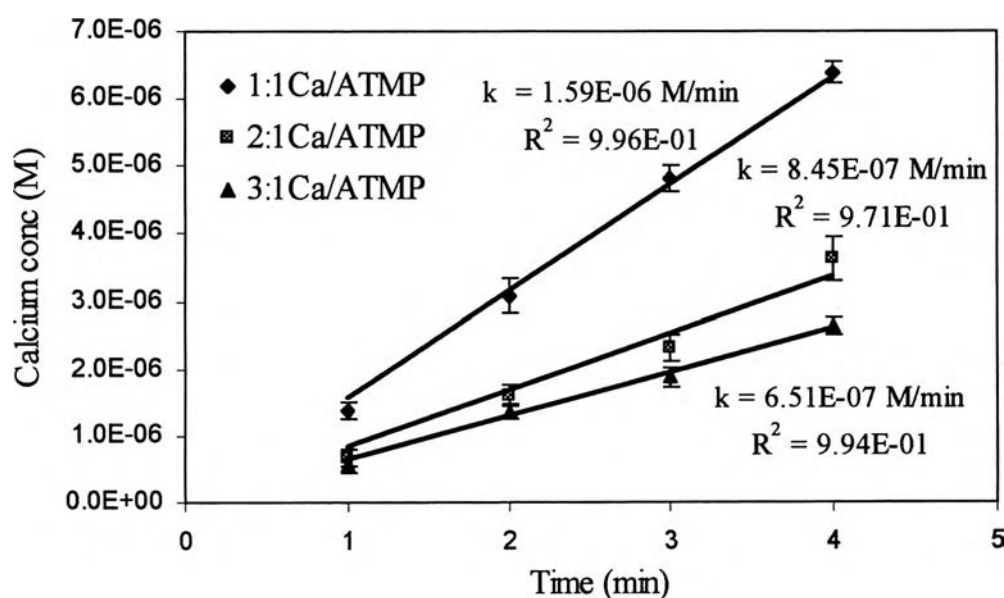


Figure 4.20 Batch dissolution of Ca/ATMP precipitates in DI water.

It is apparent that 1:1 Ca/ATMP precipitate had the highest initial dissolution rate, while the initial rate of 2:1 Ca/ATMP precipitate was greater than 3:1Ca/ATMP precipitate. These results are related with the solubility limit of precipitates measured by Rerkpattanapipat (1996). This previous work showed that the driving force for precipitate dissolution of the 1:1 precipitate was higher than the ones for the 2:1 and 3:1 precipitates. Consequently, the dissolution rate of 1:1 Ca/ATMP precipitates was the highest.

4.2.2 Dissolution Rates of Mg-ATMP Precipitates

It was found that a pellet of 1:1 Mg/ATMP precipitate was being dissolved instantly in deionized water at $t = 0$ min causing a sudden change in surface area, therefore, 1:1 Mg/ATMP precipitate was excluded from the dissolution study. The dissolution results of 2:1 and 3:1 Mg/ATMP precipitates synthesized using NaCl are illustrated in Figure 4.21

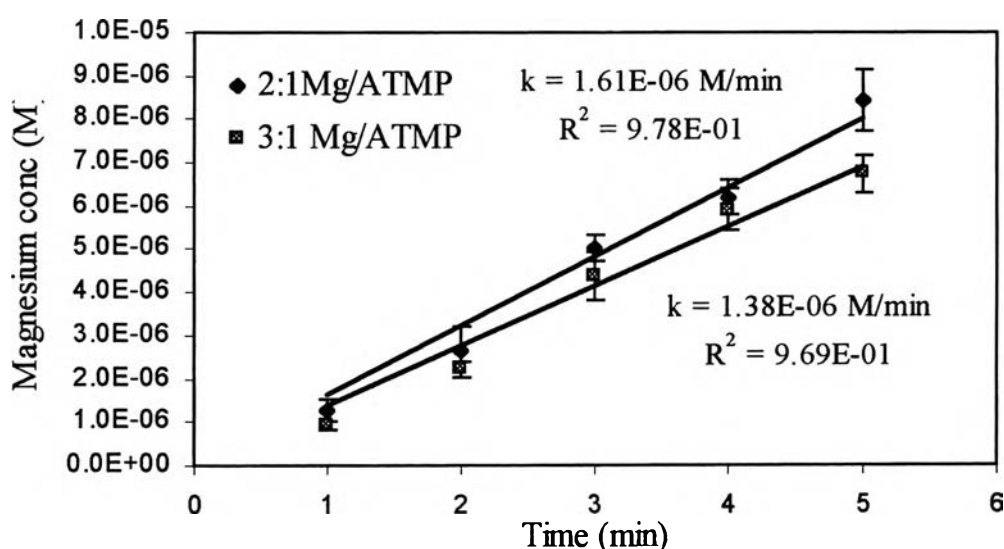


Figure 4.21 Batch dissolution of Mg/ATMP precipitates in DI water.

From Figure 4.21, 2:1 Mg/ATMP precipitate has a higher dissolution rate than 3:1 Mg/ATMP precipitate. This phenomenon can be explained in a similar manner as the batch dissolution results of Ca-ATMP

precipitates. The results also clearly showed that the initial rates of 2:1 and 3:1 Mg/ATMP precipitates were approximately greater two times than those of 2:1 and 3:1 Ca/ATMP precipitates.

4.2.3 Dissolution Rates of Mixed Precipitates

In this part, two resulting precipitates formed between ATMP with both calcium and magnesium were chosen as a model for evaluating the dissolution performance and proving the proposal hypothesis of precipitation mechanism as described before. Figures 4.22 and 4.23 demonstrate the dissolution characteristics of the two precipitates containing both calcium and magnesium ion which were formed from the solution containing the total Ca/Mg molar ratio of approximate 1:1 formed at the precipitating solution pHs of 4 and 7, respectively.

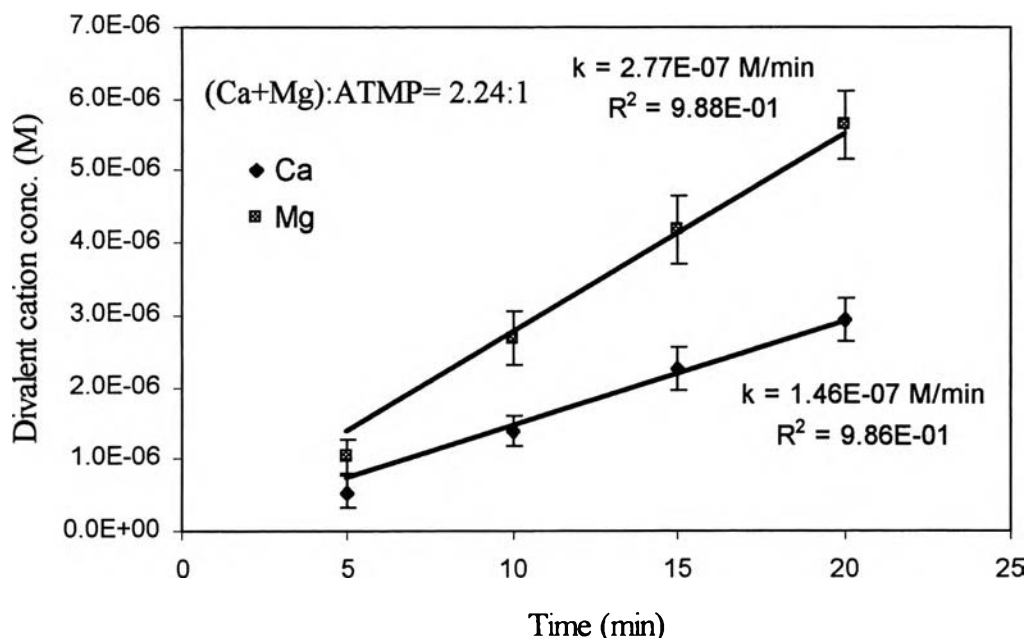


Figure 4.22 Initial dissolution rates of Mg and Ca released from the precipitate having total molar ratio of 2:1 and total Ca/Mg molar ratio of approximate 1:1 formed at precipitating solution pH of 4.

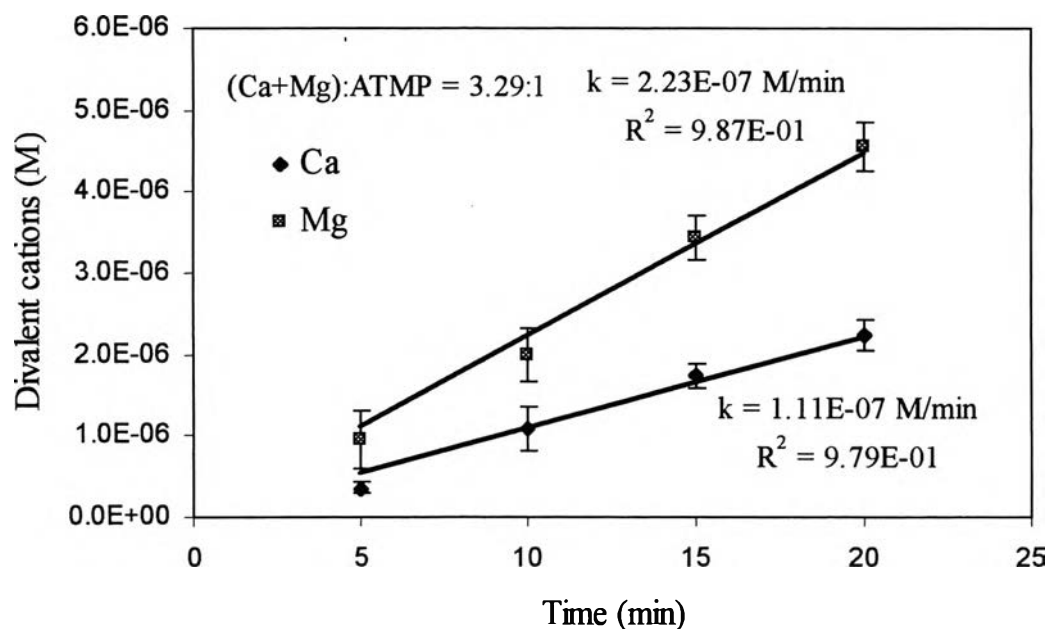


Figure 4.23 Initial rate of Mg and Ca released from precipitates having total molar ratio of 3:1 and total Ca/Mg molar ratio of approximate 1:1 formed at precipitating solution pH of 7.

It was seen obviously that the dissolution of both studied precipitates having the total Ca/Mg molar ratio of approximate 1:1 offered higher initial rates of magnesium release than those of calcium release. In addition, the initial dissolution rates of magnesium release were also approximately two times greater than those of calcium release.

Table 4.5 shows the summary of the dissolution rates of three distinct types of the precipitates which were pure Ca-ATMP precipitates, pure Mg-ATMP precipitates and the precipitates containing both calcium and magnesium ion.

Table 4.5 Summary of the dissolution rates of three types of the precipitates.

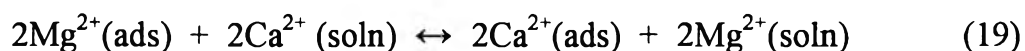
Precipitate's types	Initial dissolution rates ($\mu\text{mol}/\text{dm}^3 \cdot \text{min}$)		
	R_{Mg}	R_{Ca}	$R_{\text{Mg}}/R_{\text{Ca}}$
2:1 Mg/ATMP precipitate	1.610	-	} 1.905
2:1 Ca/ATMP precipitate	-	0.845	
3:1 Mg/ATMP precipitate	1.380	-	} 2.120
3:1 Ca/ATMP precipitate	-	0.651	
2:1 (Ca+Mg)/ATMP precipitate	0.277	0.146	1.897
3:1 (Ca+Mg)/ATMP precipitate	0.223	0.111	2.009

By comparing the same divalent cation to ATMP molar ratio in the resulting precipitates, the rate of magnesium release from 2:1 Mg/ATMP precipitate was higher than that of 2:1 Ca/ATMP precipitate with the factor of approximate two as well as the comparison between 3:1 Mg/ATMP and 3:1 Ca/ATMP precipitate. For two precipitates containing both calcium and magnesium ions and having total molar ratios of (Ca+Mg)/ATMP of 2:1 and 3:1, the similar results were obtained because magnesium ion was dissolved faster than calcium ion with the factor of around two as well. These results were good agreements with the results from the individual precipitates. These both precipitates were the mixtures of the Ca-ATMP and Mg-ATMP precipitates resulting in the separating release of calcium and magnesium ion, or in other word, magnesium ion could be able to co-precipitate along with the Ca-ATMP precipitates forming the mixed precipitates under the same precipitating conditions.

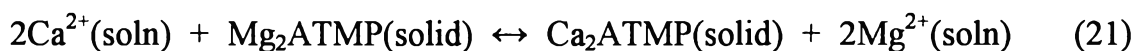
Theoretically, co-precipitation may occur by either adsorption of one material by another, or formation of a solid in another as a function of the mutual compatibility of ions within the lattice. Furthermore, the minor

component must be free to diffuse throughout the host matrix containing of major component. Under the conditions of free diffusion and compatibility of impurity with the host lattice, mixed solid precipitates are formal to form.

According to the results shown in Table 4.3, the following co-precipitation reactions for 2:1 precipitates are possibly proposed as an example. The replacement of cations within the solid may be regarded as a two-step process involving surface adsorption, followed by incorporation into the substrate lattice via free diffusion.



These reactions would be equally general for incorporation of cations. The overall equilibrium in equation (19) and (20) is given by



This overall equilibrium reaction was a good representative for explaining the phenomena shown in Figure 4.10. From this Figure, a decrease of total Ca/Mg molar ratio in the system resulted in a decrease of total Ca/Mg molar ratio in the resulting precipitate as well. Using this overall equilibrium reaction can describe that the equilibrium reaction was shifted to the left hand side with increasing the total magnesium concentration in the systems (total Ca/Mg molar ratio in the systems decreased). As a result, the amount of Mg-ATMP precipitates participated in the resulting precipitates increased, however the total molar ratio in the resulting precipitates did not change. Therefore, the amount of each precipitates strongly depends on the total concentration of both divalent cations.